The EMBO Journal (2010) 29, 2915–2929 | © 2010 European Molecular Biology Organization | All Rights Reserved 0261-4189/10
www.embojournal.org

THE EMBO JOURNAL

An MEK-cofilin signalling module controls migration of human T cells in 3D but not 2D environments

Martin Klemke[1,*], Elisabeth Kramer[1], Mathias H Konstandin[1,2], Guido H Wabnitz[1] and Yvonne Samstag[1]

[1]Institute for Immunology, University of Heidelberg, Heidelberg, Germany and [2]Department of Cardiology, University of Heidelberg, Heidelberg, Germany

T cells infiltrate peripheral tissues to execute immunosurveillance and effector functions. For this purpose, T cells first migrate on the two-dimensional (2D) surface of endothelial cells to undergo transendothelial migration. Then they change their mode of movement to undergo migration within the three-dimensional (3D)-extracellular matrix of the infiltrated tissue. As yet, no molecular mechanisms are known, which control migration exclusively in either 2D or 3D environments. Here, we describe a signalling module that controls T-cell chemotaxis specifically in 3D environments. In chemotaxing T cells, Ras activity is spatially restricted to the lamellipodium. There, Ras initiates activation of MEK, which in turn inhibits LIM-kinase 1 activity, thereby allowing dephosphorylation of the F-actin-remodelling protein cofilin. Interference with this MEK-cofilin module by either inhibition of MEK or by knockdown of cofilin reduces speed and directionality of chemotactic migration in 3D-extracellular matrices, but not on 2D substrates. This MEK-cofilin module may have an important function in the tissue positioning of T cells during an immune response.

The EMBO Journal (2010) **29,** 2915–2929. doi:10.1038/emboj.2010.153; Published online 30 July 2010
Subject Categories: cell & tissue architecture; immunology
Keywords: actin cytoskeleton; cell migration; chemotaxis; cofilin; extracellular matrix

Introduction

T cells are highly mobile cells constantly migrating into and within lymphoid and peripheral tissues. To infiltrate tissues, T cells have to leave the blood stream and to cross the endothelial cell layer, which constitutes the inner wall of blood vessels (Ley *et al*, 2007). Thus, during trafficking through the body, T cells have to migrate on two-dimensional (2D) surfaces, such as endothelial cell layers, as well as through three-dimensional (3D) interstitial extracellular matrix (ECM) tissues. T-cell migration in general is characterized by polarized cell morphology ('hand-mirror like'), relatively weak and short-lived integrin-based contacts with the substrate, rapid oscillatory shape changes mediated by the actomyosin system, and high velocity. This mode of migration has been termed 'amoeboid' migration (reviewed in Friedl *et al*, 2001; Friedl and Weigelin, 2008). Amoeboid migration can be described as a repeated four-step cycle: generation of a membrane protrusion by actin flow at the leading edge, formation of new attachments to the substrate, contraction of the cell body by the actomyosin system and finally forward movement of the rear. Depending on the environment, T cells adapt this migration programme. For migration on 2D surfaces, T cells use the above-described basic migration programme (Ley *et al*, 2007). In contrast, in 3D environments, such as interstitial ECM tissues, T cells migrate in an integrin-independent manner, in which forward movement is mainly driven by constant actin flow (Friedl *et al*, 1998; Wolf *et al*, 2003; Woolf *et al*, 2007; Lammermann *et al*, 2008). During migration in 3D ECM tissues, T cells constantly adapt their shape to the given structure of the interstitial ECM and follow the path of least resistance, a process termed 'contact guidance' (Wolf *et al*, 2003). Here, the actomyosin system is only required to squeeze the cell through narrow gaps (Lammermann *et al*, 2008).

Amoeboid migration of T cells is induced by chemokines, which bind to and signal through G-protein-coupled receptors (GPCRs) (Campbell *et al*, 2003; von Andrian and Mempel, 2003; Thelen and Stein, 2008). Most of the GPCRs in T cells transmit their signals through the Pertussis toxin (PTx)-sensitive heterotrimeric G-protein G_i. Triggering of GPCRs by chemokines leads to the activation of multiple signalling pathways culminating in the formation of a polarized cell shape, and finally cell migration along the chemokine gradient (Affolter and Weijer, 2005; Thelen and Stein, 2008). During cell polarization and migration, substantial reconstruction of the actin cytoskeleton occurs, and thus many GPCR signalling pathways act on actin-binding proteins (Samstag *et al*, 2003; Affolter and Weijer, 2005). For instance, GPCR-mediated activation of the nucleotide exchange factor DOCK-2 leads to the activation of the small GTPase Rac (Nombela-Arrieta *et al*, 2004), which induces actin polymerization at the leading edge through WAVE and Arp2/3 (Machesky *et al*, 1999; Ibarra *et al*, 2005). However, to enable constant actin flow at the leading edge, filamentous actin (F-actin) has to be simultaneously disintegrated at the rear of the lamellipodium. This is achieved by severing and depolymerization of F-actin. Severing generates new free barbed ends for the addition of globular monomeric actin (G-actin), whereas depolymerization removes actin monomers from the pointed ends, thereby providing G-actin for the addition to free barbed ends, hence increasing actin turnover rates (Pantaloni *et al*, 2001; Pollard and Borisy, 2003).

*Corresponding author. Institute for Immunology, University of Heidelberg, Im Neuenheimer Feld 305, Heidelberg 69120, Germany. Tel.: +49 6221 56 4058; Fax: +49 6221 56 5549;
E-mail: klemke@uni-heidelberg.de

Received: 22 December 2009; accepted: 14 June 2010; published online: 30 July 2010

One of the major F-actin severing and depolymerizing proteins in mammalian cells is the actin-binding protein cofilin (Lappalainen and Drubin, 1997; Theriot, 1997; Condeelis, 2001; Hotulainen *et al*, 2005; Kiuchi *et al*, 2007). In untransformed human T cells, cofilin is constitutively phosphorylated at Ser3, for example by LIM-kinases (LIMKs) (Arber *et al*, 1998; Yang *et al*, 1998), which reduces its actin-binding capacity (Moriyama *et al*, 1996). Recently, it was reported that association of HIV-1 Nef with PAK2 induces cofilin phosphorylation and inhibits the motility of fibroblasts and the chemotaxis of HIV-1-infected primary human T cells (Stolp *et al*, 2009). Dephosphorylation of cofilin at Ser3, for example by the slingshot phosphatase (Niwa *et al*, 2002) or by the phosphatases PP1 and PP2A (Ambach *et al*, 2000), induces association of cofilin with the actin cytoskeleton (Lee *et al*, 2000). Inhibition of the interaction of cofilin with actin by cell-permeable-cofilin peptide homologues in human T cells results in impaired formation of the immune synapse, reduced cytokine production and less cell proliferation (Eibert *et al*, 2004). Cofilin, therefore, represents a central integrator of T-cell activation.

Here, we show that an MEK-cofilin signalling module has an important function for the migration of human T cells in 3D environments, whereas T-cell migration on 2D substrates seems cofilin independent.

Results

Cofilin colocalizes with both dynamic and stable F-actin structures in amoeboid migrating primary human T cells

To investigate the function cofilin has during amoeboid T-cell migration, we first analysed the subcellular distribution of cofilin and its colocalization with F-actin structures in migrating human T cells. To this end, we induced amoeboid migration on ICAM-1-coated coverslips by triggering the chemokine receptor CXCR4 with its ligand SDF-1α. The chemokine receptor CXCR4 is a prototypic homeostatic chemokine receptor, and its ligand SDF-1α is secreted by a variety of tissues (reviewed in Kucia *et al*, 2005). Probing F-actin with fluorescently labelled Phalloidin revealed that at the leading edge (lamellipodium), short F-actin structures predominate (Figure 1A, lamellipodium), indicative for dynamic remodelling and high turnover of F-actin. In contrast, in the mid-zone and the uropod, long cortical F-actin structures predominate (Figure 1A, cortical F-actin, uropod), supporting cellular lateral rigidity and the integrity of the uropod. Analysis of the subcellular distribution of cofilin in migrating polarized T cells showed that cofilin colocalizes not only with short F-actin structures in the lamellipodium (Figure 1B, enlarged region), but also with the stable cortical F-actin structures in the mid-zone and the uropod (Figure 1B). The distribution of cofilin, F-actin and ICAM-3 along the front–back axis of polarized T cells was determined by a line-scan analysis (Figure 1C and D). This analysis confirmed that cofilin localized to the cell front, the mid-zone and the uropod. These data were confirmed in a high number of polarized human T cells by multispectral imaging flow cytometry (Supplementary Figure S1A–D). The incomplete colocalization of cofilin with the uropod marker ICAM-3 is most likely due to the fact that ICAM-3 is a membrane protein and, therefore, cannot fully colocalize with the cytosolic protein cofilin. Note that all proteins analysed were evenly distributed in the absence of SDF-1α (Supplementary Figure S2A). Taken together, these data show that in polarized primary human T cells, cofilin colocalizes with both dynamic F-actin structures at the cell front and stable cortical F-actin structures at the mid-zone and the uropod.

An Ras-MEK pathway mediates dephosphorylation of cofilin after chemokine receptor triggering in primary human T cells

Next, we determined whether chemokine receptor triggering leads to dephosphorylation, and thus activation, of cofilin in human T cells. Indeed, triggering of the chemokine receptor CXCR4 with its ligand SDF-1α led to dephosphorylation of cofilin over time (Figure 2A and B). Then, we investigated the signalling cascade mediating this chemokine-induced dephosphorylation of cofilin. As expected, triggering of CXCR4 with its ligand SDF-1α led to a rapid activation of Ras (Figure 2C, upper panel). This activation could be blocked by pre-incubation of the cells with PTx (Figure 2C, lower panel), indicating the involvement of the PTx-sensitive G-protein G_i upstream of Ras. Activation of Ras after SDF-1α stimulation was accompanied by activation of the kinases MEK (as shown by phosphorylation of its substrate ERK) and PI3K (as shown by phosphorylation of its substrate Akt) (Figure 2E); both events could likewise be blocked by PTx (Figure 2E). Incubation of the cells with PTx also completely blocked chemokine-induced dephosphorylation of cofilin (Figure 2E and F). To analyse, whether Ras was responsible for the activation of MEK, PI3K and dephosphorylation of cofilin after chemokine receptor triggering, we transfected primary human T cells with a cDNA coding for EGFP-tagged dominant-negative N17-Ras, and, as a control, with a cDNA coding for EGFP only. Both proteins were expressed at equal levels (Supplementary Figure S3A). The influence on the activation of MEK, PI3K and dephosphorylation of cofilin was analysed in EGFP-positive cells using flow cytometric detection of pERK, pAKT and p-Ser3-cofilin. Following stimulation with the chemokine SDF-1α, expression of N17-Ras prevented the activation of MEK (indicated by a reduced phosphorylation of its substrate ERK; Figure 2D, left panel) as well as dephosphorylation of cofilin (Figure 2D, right panel) as compared with expression of the EGFP control. In contrast, the activation of PI3K (indicated by phosphorylation of its substrate Akt) was not significantly inhibited by the expression of N17-Ras as compared with expression of the EGFP control (Figure 2D, middle panel). Accordingly, inhibition of MEK with its specific inhibitors U0126 (Figure 2E and F) or PD98059 (Supplementary Figure S4A) abolished chemokine-induced dephosphorylation of cofilin, whereas inhibition of PI3K with its specific inhibitor Ly294002 (Figure 2E and F) did not. Thus, in primary human T cells, chemokine-triggered dephosphorylation of cofilin is mediated by the G_i-induced activation of an Ras-MEK pathway.

MEK inhibits LIMK1 activity upon chemokine receptor triggering in primary human T cells thereby enhancing dephosphorylation of cofilin through phosphatase PP2A

There are hints from other cell systems that Ras-MEK negatively regulates LIMK (Lee and Helfman, 2004), and thus we investigated whether SDF-1α-induced activation of MEK negatively regulates LIMK1 in human T cells. LIMK1 activity

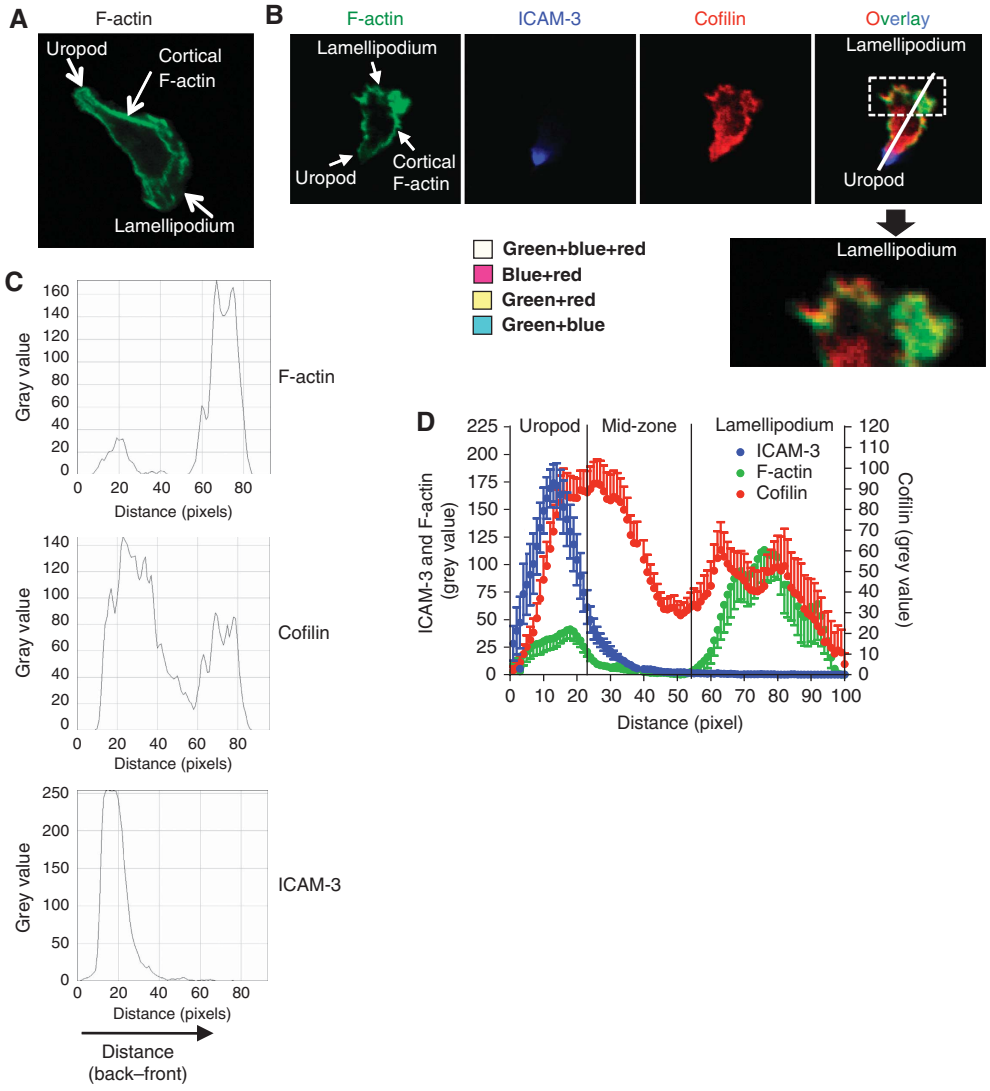

Figure 1 Cofilin colocalizes with both dynamic and stable F-actin structures in migrating primary human T cells. (**A**, **B**). Confocal microscopy of representative T cells migrating on an ICAM-1-coated coverslip upon the addition of SDF-1α. A single optical *x*–*y* section close to the level of the coverslip is shown. (**A**) F-actin was visualized with fluorescently labelled Phalloidin. (**B**) F-actin was stained with Phalloidin (green), the uropod was stained with anti-ICAM-3 (blue) and cofilin was visualized with a polyclonal anti-cofilin antiserum (red). The white box marks the enlarged area depicting the lamellipodium. (**C**) Fluorescence intensity distribution (grey values) across the back–front axis (depicted by the white line in (**B**)) of the cell shown in (**B**). (**D**) Fluorescence intensity distribution across the back–front axis of multiple polarized T cells. The mean grey values ± s.d. are shown ($n = 14$).

is induced by phosphorylation of Thr508 within its activation loop (Ohashi *et al*, 2000). Interestingly, upon SDF-1α stimulation, LIMK1 was rapidly dephosphorylated at Thr508 (Figure 3A and B, no inhibitor), and thus inactivated. Pretreatment of T cells with the MEK inhibitor U0126 prevented dephosphorylation of LIMK1 upon SDF-1α stimulation (Figure 3A and B, U0126). We (Ambach *et al*, 2000) and others (Quintela-Fandino *et al*, 2010) have shown that the serine/threonine-phosphatase PP2A associates with and dephosphorylates cofilin. Indeed, the phosphatase inhibitor Okadaic acid (which at the concentration used inhibited PP2A, but not PP1 (data not shown)) blocked dephosphorylation of cofilin upon SDF-1α stimulation (Figure 3C and D). PP2A is negatively regulated by phosphorylation of Tyr307 at its catalytic subunit, and active PP2A prevents phosphorylation at Tyr307 by auto-dephosphorylation (Chen *et al*, 1992). Interestingly, phosphorylation of Tyr307 of PP2A could not be detected in resting human T cells (Figure 3E, untreated), indicating that PP2A is constitutively active. However, phosphorylation of Tyr307 could be detected upon treatment of resting T cells with Okadaic acid (Figure 3E), indicating inhibition of PP2A. These results suggest that both LIMK1 and PP2A are constitutively active in resting human T cells and maintain a certain balance between phosphorylated and dephosphorylated cofilin.

To prove this, we modulated the LIMK1 phosphorylation status—and thus LIMK1 activity—in resting human T cells by inhibition of ROCK, which directly activates LIMK1 by phosphorylation of Thr508 (Ohashi *et al*, 2000). Inhibition of ROCK by its specific inhibitor Y-27632 indeed reduced LIMK1 activity (Supplementary Figure S5A) and lowered the level of P-Ser3-cofilin in resting human T cells (Supplementary Figure S5B). This effect could in part be compensated by inhibition of PP2A with Okadaic acid (Supplementary Figure S5B).

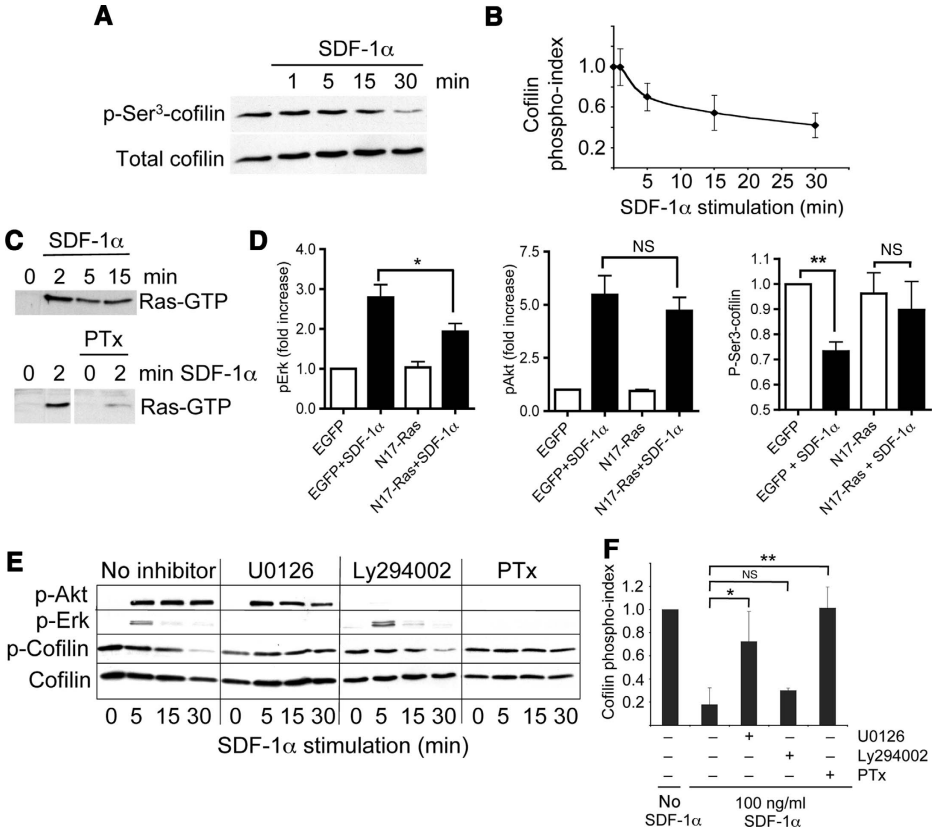

Figure 2 An Ras-MEK pathway mediates dephosphorylation of cofilin after chemokine receptor triggering in human T cells. (**A**) Primary human T cells were incubated in the absence or presence of SDF-1α for the indicated time points. Cells were lysed and phosphorylated cofilin (p-Ser3-cofilin) and total cofilin were detected by immunoblotting. Shown is one representative experiment out of three. (**B**) The levels of phospho-cofilin and total cofilin were detected by immunoblotting as described above, and the cofilin phospho-index was calculated. The mean values ± s.d. of three independent experiments are shown. (**C**) Human T cells were incubated in the absence (upper blot) or presence of Pertussis toxin (PTx, lower blot). Cells were then stimulated with SDF-1α for the indicated time points, lysed and Ras-GTP was precipitated from the lysate with RBD agarose and detected by immunoblotting using an antibody against human Ras. Shown is one representative experiment out of three. (**D**) Human T cells were transfected either with a cDNA encoding EGFP (EGFP), or with a cDNA encoding an EGFP-fusion protein of dominant-negative Ras (N17-Ras). T cells were incubated in the presence or absence of SDF-1α for 2 min (pERK, pAKT) or 30 min (p-Ser3-cofilin). Then, cells were fixed, permeabilized and stained with either a phospho-Erk (left panel) or a phospho-Akt (middle panel) PE-labelled antibody. P-cofilin was detected with a P-Ser3-cofilin antiserum and PE-conjugated secondary antibodies (right panel). The mean fluorescence intensity for PE of EGFP-positive cells was determined by flow cytometry (see Supplementary Figure S3B). The values obtained for EGFP-transfected cells in the absence of SDF-1α were set 1 and all other values were expressed relative to them. The mean values ± s.d. of three independent experiments are shown. $*P<0.05$; $**P<0.01$; NS, not significant. (**E**) Human T cells were either not treated (no inhibitor) or treated with the indicated inhibitors. Afterwards, cells were incubated in the absence or presence of SDF-1α for the indicated time points and the levels of phospho-cofilin and total cofilin were detected by immunoblotting. In addition, the same blots were probed with two different antisera detecting the phosphorylated forms of Akt and Erk, respectively. Shown is one representative experiment out of three. (**F**) Human T cells were treated as in (**E**). The levels of phospho-cofilin and total cofilin were detected by immunoblotting, and the cofilin phospho-index was calculated. The mean values ± s.d. of three independent experiments are shown. $*P<0.05$; $**P<0.01$; NS, not significant.

Thus, we conclude that SDF-1α activates MEK, and MEK in turn leads to inhibition of LIMK1, which then shifts the balance towards dephosphorylation of cofilin.

GTPase Ras is specifically activated at the leading edge of migrating primary human T cells

It was a puzzling finding that during amoeboid T-cell migration the actin-remodelling protein cofilin is not only exclusively localized to dynamic F-actin structures, for example at the leading edge, but is also found at sites of stable F-actin structures needed for cellular rigidity, for example the cortical F-actin in the mid-zone (see Figure 1). It is, therefore, likely that in migrating T cells, activation of cofilin occurs in a compartmentalized way, being restricted to sites of F-actin reconstruction. The signal transduction cascade mediating the activation of cofilin after chemokine receptor triggering in human T cells is initiated by the GTPase Ras (see Figure 2). To investigate a spatially restricted activation of Ras in migrating T cells, we took advantage of a sensor specific for GTP-bound active Ras. This sensor consists of the EGFP-tagged Ras-binding domain (RBD) of human c-Raf-1. The RBD of Raf-1 interacts specifically with GTP-bound active Ras (Herrmann *et al*, 1995), and its EGFP-tagged version (EGFP-Raf-RBD) can be used to probe activation of Ras within living cells (Sasaki *et al*, 2004). Thus, we transfected primary human T cells with EGFP-Raf-RBD and, as a control, with EGFP alone (Supplementary Figure S3C and D). Cell migration on ICAM-1-coated coverslips was induced by the addition of the chemokine SDF-1α, and the subcellular localization of EGFP-Raf-RBD in polarized migrating T cells was analysed by confocal microscopy. Full polarization of T cells was assured by the exclusive localization of ICAM-3 to the uropod

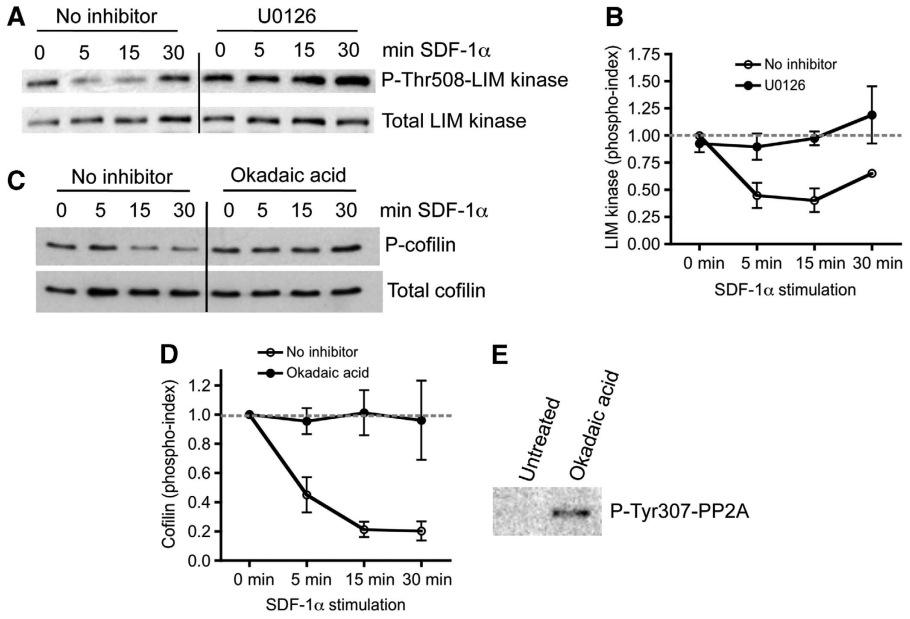

Figure 3 MEK inhibits LIMK1 activity upon chemokine receptor triggering in primary human T cells, thereby enhancing dephosphorylation of cofilin through phosphatase PP2A. (**A**) T cells were pre-treated or not with the MEK-inhibitor U0126, and then incubated in the absence or presence of SDF-1α for the indicated time points. Cells were lysed and phosphorylated LIMK1 (p-Thr508-LIM kinase) and total LIMK1 were detected by immunoblotting. Shown is one representative experiment out of three. (**B**) The levels of phospho-LIMK1 and total LIMK1 were detected by immunoblotting as described above, and the LIMK1 phospho-index was calculated. The mean values ± s.d. of three independent experiments are shown. (**C**) Primary human T cells were pre-treated or not with Okadaic acid and incubated in the absence or presence of SDF-1α for the indicated time points. Cells were lysed and phosphorylated cofilin (p-Ser3-cofilin) and total cofilin were detected by immunoblotting. Shown is one representative experiment out of three. (**D**) The levels of phospho-cofilin and total cofilin were detected by immunoblotting as described above, and the cofilin phospho-index was calculated. The mean values ± s.d. of three independent experiments are shown. (**E**) Resting human T cells were either left untreated or were treated with Okadaic acid. Cells were lysed and phosphorylated PP2A (P-Tyr307-PP2A) was detected by immunoblotting. Shown is one representative experiment out of three.

(Figure 4A, upper panels). The EGFP control shows no enrichment at the leading edge of migrating T cells (Figure 4A, left column). In marked contrast, EGFP-Raf-RBD was strongly enriched at the leading edge of migrating T cells (Figure 4A; right columns) where also cofilin is localized. Only little EGFP-Raf-RBD was found in the mid-zone and the uropod. Note that in the absence of SDF-1α, EGFP-Raf-RBD was evenly distributed within the cell (Supplementary Figure S2A). These data indicate that Ras activity is concentrated within the lamellipodium of migrating T cells. Hence, activation of the Ras-MEK pathway, and thus dephosphorylation of cofilin, should occur especially at the lamellipodium. Indeed, in contrast to total cofilin (Figure 4B, cofilin), only little phosphorylated cofilin could be detected in the lamellipodium (Figure 4B, pSer3-cofilin). Calculation of the ratio of phosphorylated versus total cofilin (see Supplementary Figure S2B) revealed that this ratio is much lower within the lamellipodium compared with the rest of the cell (Figure 4C). Thus, although cofilin is found throughout the whole cytoplasm of migrating T cells (Figures 1B and 4B), its dephosphorylation occurs mainly at the lamellipodium.

T cells do not only migrate on 2D surfaces, for example endothelial cells, but also migrate within the interstitial space of tissues, where they face the 3D environment of the ECM. The 2D migration is mainly driven by actin-myosin contractions (see Supplementary Movie M1). In contrast, 3D migration is characterized by flowing and squeezing of the cell (see Supplementary Movies M2 and M3), which is mainly driven by actin flow. The functions Ras, MEK and cofilin have in these two types of amoeboid T-cell migration have not been investigated so far. Thus, we systematically interfered with each of the three molecules and analysed migration in both 2D and 3D environments.

Interference with Ras activity impairs chemotactic migration of primary human T cells in both 2D and 3D environments by reducing speed and directionality

To obtain information about the function of Ras in T-cell migration, we again transfected primary human T cells with EGFP-tagged dominant-negative N17-Ras. Then, T cells were allowed to migrate across transwell inserts in the absence or presence of an SDF-1α gradient under either 2D or 3D conditions. For 2D transmigration, transwell inserts were coated on their upper surface with ICAM-1. Thus, T cells first had to migrate on the planar surface of the transwell insert before they could reach a pore and finally transmigrate (see Supplementary Figure S6A). To investigate 3D T-cell transmigration, transwell inserts were overlaid with a 3D layer of Matrigel. This ECM mixture forms a complex gel and can be used as a model system for chemotactic migration of leukocytes, including T cells, in a 3D environment (Loike *et al*, 2001; Zheng *et al*, 2001). Here, T cells first had to migrate within this 3D environment before they could reach a pore of the transwell insert to finally undergo transmigration (see Supplementary Figure S6B).

Expression of EGFP-tagged dominant-negative N17-Ras in primary human T cells reduced their chemotactic migration in the 2D-transmigration assay (Figure 5A) as well as the 3D-transmigration assay (Figure 5F). Interestingly, this

inhibitory effect of N17-Ras expression on chemotactic transmigration was much more pronounced in the 3D-transmigration assay. Transwell migration assays permit bulk analysis of cell migration. To track individual T cells, we took advantage of time-lapse videomicroscopy. To this end, 2D- and 3D-chemotactic migration was carried out as described above, and tracks of individual migrating T cells were recorded by time-lapse videomicroscopy. EGFP-expressing control T cells displayed directed movement towards the source of the chemokine gradient (the pore of the transwell insert) in both 2D (Figure 5B, control; see corresponding Supplementary Movie M4) and 3D environments (Figure 5G, control; see corresponding Supplementary Movie M5). N17-Ras-expressing T cells were slightly impaired in directed move-

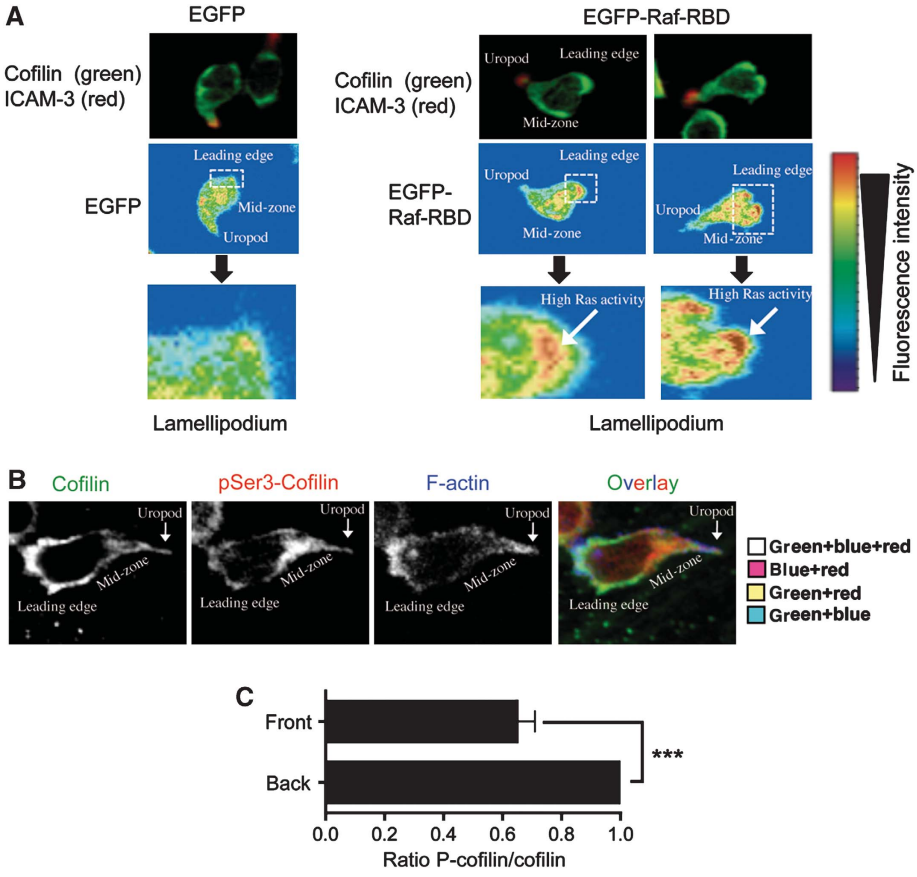

Figure 4 The GTPase Ras is specifically activated at the leading edge of migrating primary human T cells. (**A**) Primary human T cells were either transfected with a cDNA encoding EGFP (left panels) or with a cDNA encoding EGFP-Raf-RBD (right panels). Cell migration on ICAM-1-coated coverslips was induced by the addition of SDF-1α. Cells were analysed by confocal microscopy. Shown are single optical *x*–*y* sections. The uropod was stained with anti-ICAM-3 (upper panels; red), and cofilin was visualized with a polyclonal anti-cofilin antiserum (upper panels; green). The subcellular distribution of EGFP-Raf-RBD is shown by false colours (lower panels). The white boxes mark the enlarged areas depicting the lamellipodia. EGFP-Raf-RBD is enriched at the edge of the lamellipodium (white arrows). (**B**) Migration of primary human T cells on ICAM-1-coated coverslips was induced by the addition of SDF-1α. Cells were analysed by confocal microscopy. Total cofilin was detected with a mouse monoclonal antiserum (green), phospho-Ser3-cofilin was detected with a rabbit phospho-Ser3-specific antiserum (red), and F-actin was visualized with Phalloidin (blue). (**C**) The ratio of phospho-Ser3-cofilin (P-cofilin) versus total cofilin (cofilin) was determined for both the cell front and the cell back as depicted in Supplementary Figure S2D. The ratio determined for the cell back was set 1 and the ratio determined for the cell front was expressed relative to it. The mean values ± s.d. are shown ($n = 19$). $^{***}P < 0.001$.

Figure 5 Interference with Ras activity impairs chemotactic migration of human T cells in both 2D and 3D environments by reducing speed and directionality. (**A**, **F**) Human T cells were either transfected with a cDNA encoding EGFP (Control), or with a cDNA encoding an EGFP-fusion protein of dominant-negative Ras (N17-Ras). Cells were allowed to migrate either across ICAM-1-coated transwell inserts (**A**) or across a Matrigel layer on the top of a transwell insert (**F**) in the absence or presence of SDF-1α in the lower compartment. The percentages of migrated EGFP-positive cells were determined. The mean values ± s.d. of three independent experiments are shown. $^{*}P < 0.05$; $^{***}P < 0.001$. (**B**, **G**) Time-lapse videomicroscopy of primary human T cells expressing either EGFP (Control) or the N17-Ras-EGFP (N17-Ras)-fusion protein. Cells were allowed to migrate either on an ICAM-1-coated 2D surface of a transwell insert (**B**) or within a 3D-Matrigel layer on top of a transwell insert (**G**) in the presence of an SDF-1α gradient. Data are representative of three independent experiments. Tracks of the migrating T cells are shown in red. The pores of the transwell insert (source of the chemokine gradient) are labelled with numbers. The fluorescence intensity of the EGFP-expressing cells is shown by false colours. See also corresponding Supplementary Movies M4–M7. (**C**, **H**) Multiple tracks of individual human T cells. The starting points of the recorded cell tracks were artificially set to the same origin. Shown is one representative experiment out of three. (**D**, **I**) The velocities and Euclidean distances of individual human T cells were calculated from the recorded tracks. The mean values ± s.d. of three independent experiments are shown. $^{*}P < 0.05$; $^{***}P < 0.001$. (**E**, **J**) The directionality of cell migration for each condition was calculated as the Euclidean distance divided by the accumulated distance (see Supplementary Figure S6C). $^{*}P < 0.05$.

ment towards the source of the gradient in 2D migration (Figure 5B, N17-Ras; see corresponding Supplementary Movie M6). Importantly, they were strongly impaired in their directed movement towards the source of the gradient in 3D migration (Figure 5G, N17-Ras; see corresponding Supplementary Movie M7). By analysing the tracks of numerous individual cells (Figure 5C and H), we calculated the velocity, the accumulated distance and the Euclidean

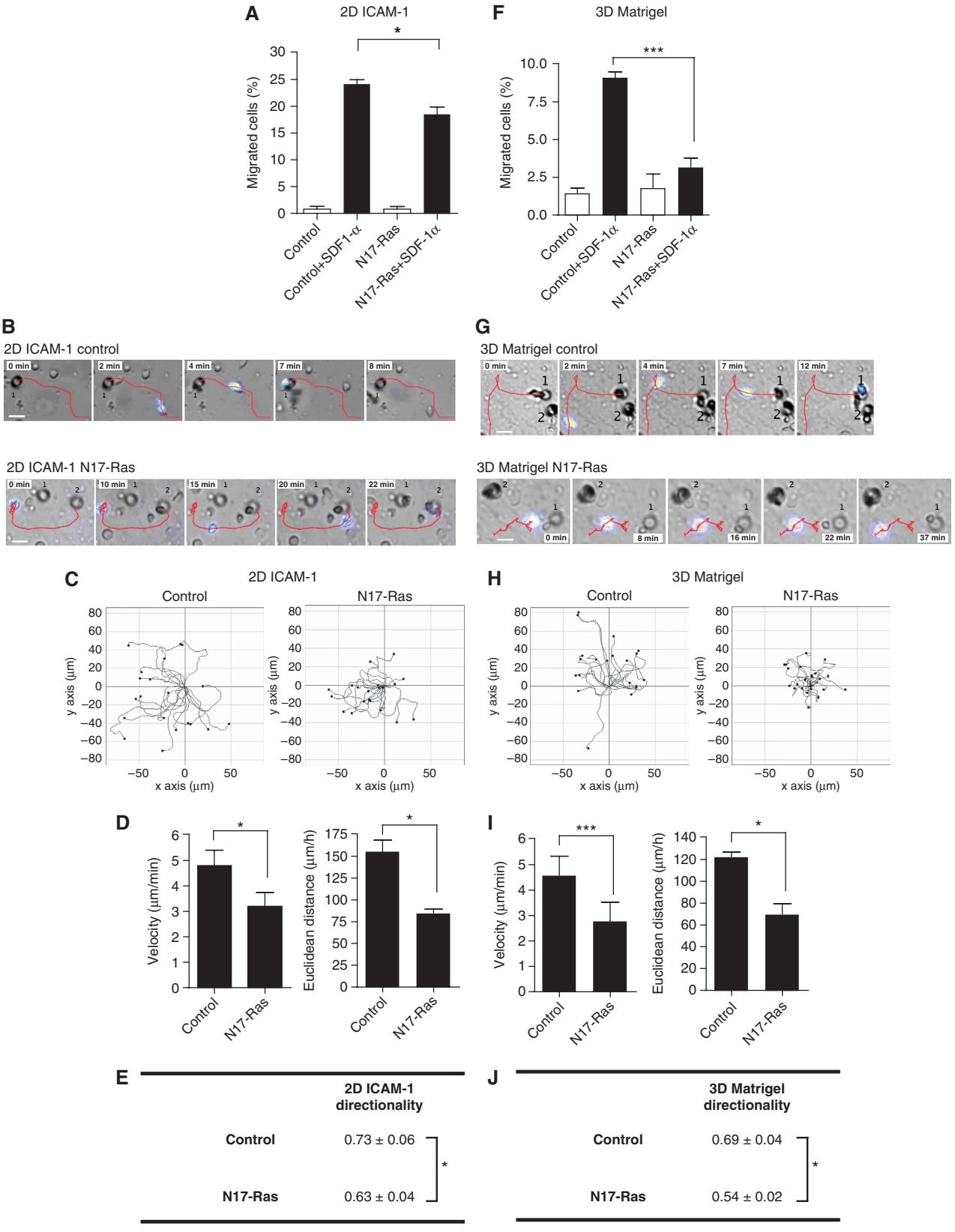

distance of cell migration. The directionality of cell movement was determined as the Euclidean distance divided by the accumulated distance (see Supplementary Figure S6C). Expression of N17-Ras resulted in a reduction in migration speed (Figure 5D, I; left), in the Euclidean distance (Figure 5D, I, right) and in the directionality of cell movement (Figure 5E and J) in both 2D and 3D environments as compared with EGFP-expressing control cells. In line with the bulk analysis of 2D- and 3D-chemotactic transmigration (Figure 5A and F), the inhibitory effect of N17-Ras on the velocity and directionality of chemotactic migration was even more pronounced in the 3D environment.

Inhibition of MEK impairs chemotactic migration of primary human T cells in 3D but not 2D environments by reducing speed and directionality

Downstream of Ras, activation of cofilin is mediated by MEK (see Figure 2). To elucidate the functional consequences of interference with MEK on T-cell migration, we pre-incubated primary human T cells with the MEK inhibitor U0126. Then, T cells were allowed to migrate across transwell inserts in the absence or presence of an SDF-1α gradient under either 2D or 3D conditions. Surprisingly, although inhibiting cofilin dephosphorylation (compare Figure 2E and F), blocking the activation of MEK by U0126 (Figure 6A) or by the structurally unrelated MEK-inhibitor PD98059 (Supplementary Figure S4B) had no effect on 2D-chemotactic transmigration. In marked contrast, pre-incubation of the T cells with either U0126 (Figure 6F) or PD98059 (Supplementary Figure S4C) considerably reduced the number of transmigrating T cells in a chemotactic 3D-transmigration assay.

To analyse individual human T cells during chemotactic migration, untreated or U0126-treated T cells were allowed to migrate on either a 2D surface (ICAM-1) or within a 3D environment (Matrigel) in the presence of an SDF-1α gradient. Cell tracks were recorded by time-lapse videomicroscopy (Figure 6B, C, G and H), and the velocity, the accumulated distance, the Euclidean distance and the directionality of cell migration were determined. This revealed that interference with MEK did not have considerable influence on chemotactic T-cell migration on 2D surfaces (Figure 6B–E; see corresponding Supplementary Movies M8 and M9). The situation was, however, completely different, when we tracked individual T cells migrating within a 3D environment. Untreated human T cells displayed rectilinear movement towards the source of the chemokine gradient (pore of the transwell insert) (Figure 6G, no inhibitor; see corresponding Supplementary Movie M10). In marked contrast, U0126-treated T cells displayed a high turning frequency and showed no directed movement towards the source of the chemokine gradient (Figure 6G, U0126; see corresponding Supplementary Movie M11). As opposed to 2D migration (Figure 6D and E), inhibition of MEK with U0126 reduced the velocity of cell movement (Figure 6I, left), the Euclidean distance (Figure 6I, right) and the directionality of cell movement (Figure 6J) in 3D environments. To exclude that these effects of MEK inhibition rely on the different substrates used (ICAM-1 for 2D and Matrigel for 3D migration), we directly compared migration of T cells on a 2D thin film of Matrigel with migration within a 3D layer of Matrigel. Also in this setting, treatment of T cells with the MEK inhibitor U0126 impaired migration only within the 3D environment, but not on the 2D surface (Supplementary Figure S7; see also corresponding Supplementary Movies M12 and M13). Thus, active MEK is specifically required for the control of speed and directionality of human T cells during 3D-chemotactic migration—not 2D migration.

Active MEK-cofilin module is required for the actin-flow-driven mode of T-cell movement

Inhibition of MEK prevents the dephosphorylation and thus activation of the F-actin-remodelling protein cofilin in primary human T cells (Figure 2). Surprisingly, this treatment inhibits only the 3D migration—not 2D migration—of human T cells. This different dependence of 2D versus 3D migration on MEK and cofilin could be explained by the fact that, in contrast to migration on 2D substrates, T-cell migration in 3D ECM gels is mainly driven by constant actin flow at the leading edge (Friedl *et al*, 1998; Wolf *et al*, 2003; Woolf *et al*, 2007; Lammermann *et al*, 2008). Constant actin flow is principally enabled by activation of cofilin, which increases the rate of depolymerization from the pointed ends of actin filaments (Lappalainen and Drubin, 1997; Theriot, 1997; Hotulainen *et al*, 2005; Kiuchi *et al*, 2007). The 2D T-cell migration is mainly driven by actin-myosin contractions, unless T cells are treated with the Myosin II-blocker Blebbistatin. This treatment forces T cells to migrate also on a 2D surface by actin flow (Jacobelli *et al*, 2009; compare corresponding Supplementary Movie M1 with Movie M14).

To provide evidence that the MEK-cofilin module is specifically involved in the actin-flow-driven mode of cell movement, we treated human T cells with Blebbistatin. Indeed, upon treatment with Blebbistatin, velocity and directionality of T cells migrating on a 2D surface was now reduced by the

Figure 6 Inhibition of MEK impairs chemotactic migration of human T cells in 3D but not 2D environments by reducing speed and directionality. (**A**, **F**) Human T cells were treated or not with the MEK-inhibitor U0126. Cells were allowed to migrate either across ICAM-1-coated transwell inserts (**A**) or across a Matrigel layer on top of a transwell insert (**F**) in the absence or presence of SDF-1α in the lower compartment. The percentages of migrated cells were determined. The mean values ± s.d. of three independent experiments are shown. NS, not significant. $^{**}P<0.01$. (**B**, **G**) Time-lapse videomicroscopy of primary human T cells migrating on either an ICAM-1-coated 2D surface of a transwell insert (**B**) or within a 3D-Matrigel layer on top of a transwell insert (**G**) in the presence of an SDF-1α gradient. Cells were either left untreated (no inhibitor), or were treated with the MEK-inhibitor U0126. Data are representative of three independent experiments. Tracks of the cells are shown in red. The pores of the transwell insert (source of the chemokine gradient) are labelled with numbers. See also corresponding Supplementary Movies M8–M11. (**C**, **H**) Multiple tracks of individual human T cells. The starting points of the recorded cell tracks were artificially set to the same origin. Shown is one representative experiment out of three. (**D**, **I**) The velocities and Euclidean distances of individual human T cells were calculated from the recorded tracks. The mean values ± s.d. of three independent experiments are shown. NS, not significant; $^{*}P<0.05$; $^{**}P<0.01$. (**E**, **J**) The directionality of cell migration for each condition was calculated as the Euclidean distance divided by the accumulated distance (see Supplementary Figure S6C). NS, not significant; $^{*}P<0.05$.

MEK inhibitor U0126 (Figure 7A and B). We conclude that the MEK-cofilin module specifically controls the actin-flow-driven mode of cell movement (normally used for T-cell migration in 3D environments), but not the contraction-based mode of cell movement (used for T-cell migration on 2D substrates).

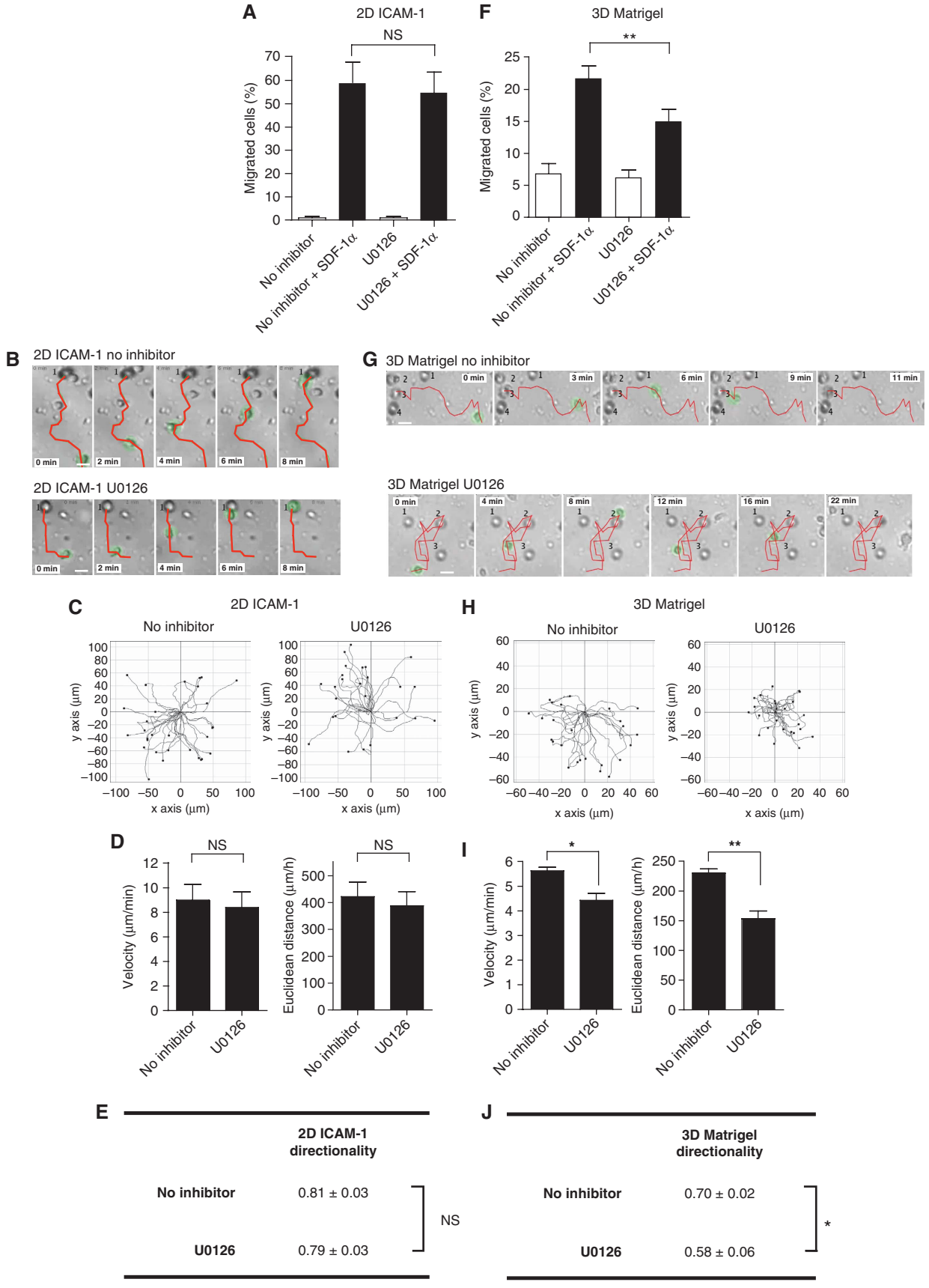

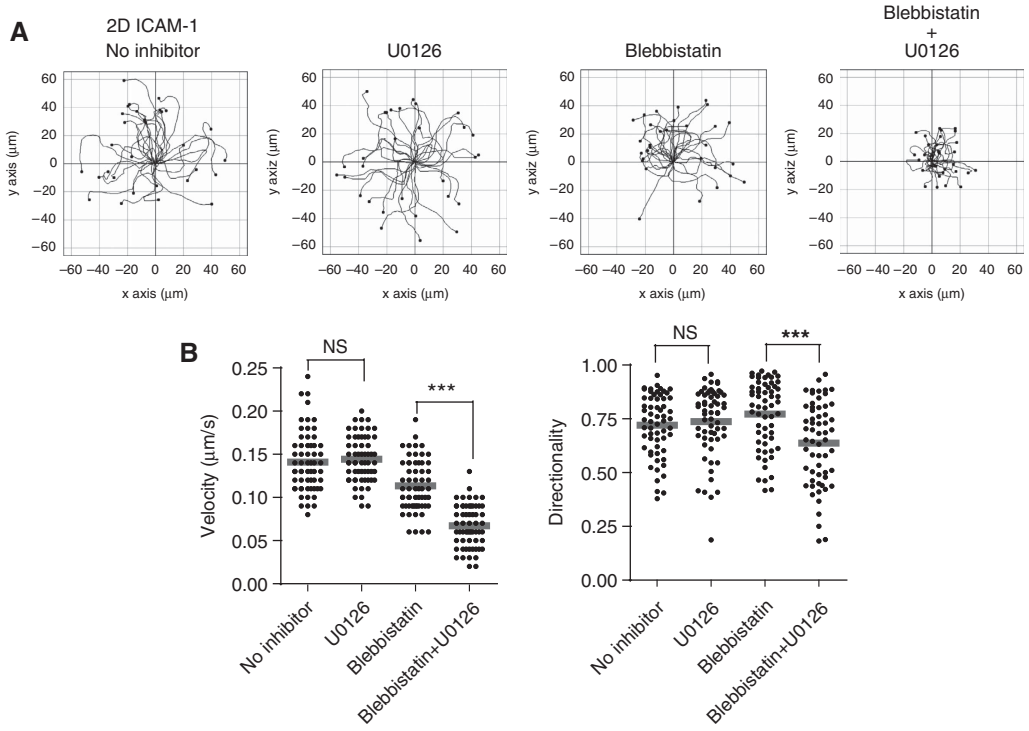

Figure 7 Active MEK is required for the actin-flow-driven mode of T-cell movement. (**A**) Primary human T cells were pre-treated or not with Blebbistatin. Cells were then allowed to migrate in the absence or presence of U0126 on the ICAM-1-coated 2D surface of a transwell insert in the presence of an SDF-1α gradient (see corresponding Supplementary Movie M14). Multiple tracks of individual T cells were recorded by time-lapse videomicroscopy. The starting points of the recorded cell tracks were artificially set to the same origin. Shown is one representative experiment out of three. (**B**) The velocities of individual human T cells were calculated from the recorded tracks (left panel), the directionalities were calculated as the Euclidean distances divided by the accumulated distances (right panel). NS, not significant; $***P<0.001$.

Knockdown of cofilin impairs chemotactic migration of human T cells in 3D but not 2D environments by reducing speed and directionality

To formally prove that cofilin activation is only required for the 3D mode of T-cell migration, we performed an siRNA-mediated knockdown of cofilin in human T cells. This resulted in 80% reduction of cofilin protein levels compared with T cells transfected with a non-targeting control siRNA (Figure 8A and B), and to a significant increase in cellular F-actin (Figure 8C) indicating that the G-actin/F-actin ratio is out of balance, if the level of the actin depolymerizing protein cofilin is lowered. In line with the functional outcome of MEK blockade (Figure 6), knockdown of cofilin had no influence on 2D-chemotactic transmigration (Figure 9A) of human T cells, but strongly inhibited 3D-chemotactic transmigration (Figure 9F).

To analyse individual siRNA-transfected T cells during chemotactic migration, time-lapse videomicroscopy was performed. Cell tracks were recorded (Figure 9B, C, G and H), and the velocity, the accumulated distance, the Euclidean distance and the directionality of cell migration were calculated. In line with the 2D-chemotactic transwell assays (Figure 9A), knockdown of cofilin neither reduced the migration speed, nor the Euclidean distance and the directionality of cell movement on a 2D surface as compared with T cells transfected with a non-targeting control siRNA (Figure 9D and E; see corresponding Supplementary Movies M15 and M16).

In a 3D microenvironment, this situation was again completely different. Thus, in 3D-migration assays T cells transfected with a control siRNA migrated in a linear way towards the source of the chemokine gradient (the pore of the transwell insert) (Figure 9G, upper panel; see corresponding Supplementary Movie M17). In marked contrast, despite the presence of a chemokine gradient, T cells transfected with the

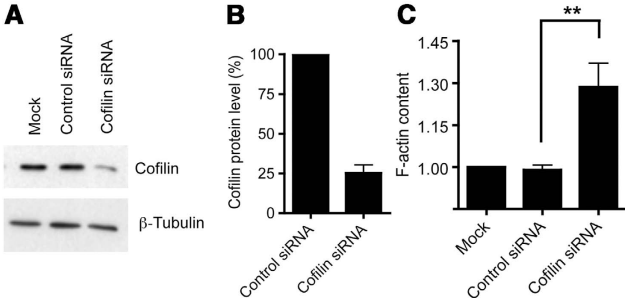

Figure 8 Knockdown of cofilin in human T cells. (**A**) Human Jurkat T cells were either transfected without siRNA (Mock), with a 'scrambled' control siRNA (Control siRNA) or with siRNA against cofilin (cofilin siRNA). Cells were lysed 72 h after transfection and the expression of cofilin and β-tubulin were analysed by immunoblotting. Shown is one representative experiment out of three. (**B**) Quantification of cofilin protein levels by densitometry. The values obtained for cells transfected with control siRNA were set 100 and the other values were expressed relative to them. The mean values ± s.d. of three independent experiments are shown. (**C**) The F-actin content was determined by flow cytometry using fluorescently labelled Phalloidin. The mean fluorescence values obtained for mock-transfected cells were set 1 and all other values were expressed relative to them. The mean values ± s.d. of three independent experiments are shown. $**P<0.01$.

cofilin-specific siRNA did either not migrate at all or migrated in a more or less random manner (Figure 9G, lower panel; see corresponding Supplementary Movie M18) during 3D-chemotactic migration. Knockdown of cofilin reduced the velocity of cell movement (Figure 9I, left), the Euclidean distance (Figure 9I, right) and the directionality of cell movement within the 3D environment (Figure 9J). Thus, knockdown of cofilin produced the same functional phenotype as inhibition of MEK. We conclude that the MEK-controlled activity of cofilin is crucial for the chemotactic migration of human T cells in 3D but not 2D environments.

Knockdown of cofilin in human T cells leads to uncontrolled formation of cell protrusions and thus to a loss of polarity in 3D environments

Morphological analysis of T cells migrating on 2D substrates showed that, despite knockdown of cofilin, migrating T cells still displayed a polarized 'hand-mirror'-like morphology (Figure 10A). This situation was completely different if T cells migrated in 3D substrates. Whilst T cells transfected with a control siRNA displayed a polarized morphology and migrated by the extension of a single lamellipodium pointing in the direction of cell movement (Figure 10B, left), knockdown of cofilin led to the formation of multiple extensions emanating from the cell body in all directions ('multidirectional irritation') (Figure 10B, right; Figure 10C; see corresponding Supplementary Movie M19), and thus to a loss of polarity. Thus, active cofilin, although not involved in induction of cell polarity (see Supplementary Figure S1E), seems to be important for the maintenance of cell polarity (a single lamellipodium at the cell front) to ensure rectilinear chemotactic movement in a 3D environment, not in a 2D environment.

Discussion

In this study, we identified a GPCR-triggered Ras-driven MEK-cofilin signalling module (Supplementary Figure S8A) that operates within the lamellipodium of amoeboid migrating primary human T cells to control directed cell movement within 3D environments (e.g. ECM tissues), but not on 2D substrates (e.g. ICAM-1 on the surface of endothelial cells). We showed that triggering of GPCRs leads to spatially restricted activation of the GTPase Ras within the lamellipodium of chemotaxing primary human T cells, which in turn induces the activation of MEK and finally dephosphorylation of cofilin. Interference with either MEK or cofilin results in a decrease in the migration speed and an increase in the turning frequency of T cells migrating in 3D environments, but not of T cells migrating on 2D substrates. This fundamental difference can be explained by the fact that T cells migrating on 2D substrates form only small lamellipodial protrusions and drive their migration mainly by contractions of the actomyosin system. Therefore, they depend only to a small extent on actin flow. In contrast, T cells migrating within ECM tissues drive their migration mainly by actin flow at the lamellipodium, and use their actomyosin-system only to squeeze themselves through narrow gaps (Friedl *et al*, 1998; Lammermann *et al*, 2008; Wolf *et al*, 2003; Woolf *et al*, 2007). Thus, under 3D conditions, it is necessary to enhance the turnover and thus depolymerization of actin filaments to maintain constant actin flow (Supplementary Figure S8B). This may be achieved by the activation of cofilin, which increases the rate of depolymerization from the pointed ends of actin filaments (Lappalainen and Drubin, 1997; Theriot, 1997; Hotulainen *et al*, 2005; Kiuchi *et al*, 2007). The special dependence of 3D migration on constant actin flow may, therefore, explain why 3D migration, in contrast to 2D migration, is sensitively and specifically blocked by the inhibition of cofilin activity. In line with the assumption that the MEK-cofilin module is crucial for migration under conditions of low G-actin levels, chemotactic migration on 2D substrates upon the inhibition of MEK was only impaired, if T cells were pre-treated with Latrunculin B and thus had low G-actin levels (Supplementary Figure S9). Interestingly, if actomyosin contractions were inhibited by the Myosin II-inhibitor Blebbistatin, T cells migrate also on a 2D surface by actin flow (Jacobelli *et al*, 2009), and their movement is then dependent on the MEK-cofilin module (see Figure 7). This finding explains why in another study a function for cofilin in the control of 2D migration could be detected (Sidani *et al*, 2007): the metastatic tumour cells analysed in this study migrate, in contrast to untransformed primary human T cells, also on 2D substrates by actin flow (similar to Blebbistatin-treated T cells). Taken together, these data suggest a function for the MEK-cofilin signalling module for the actin-flow-driven 'sliding' mode of cell movement and not for the actomyosin-driven 'walking' mode of cell movement.

The MEK-cofilin signalling module is activated by Ras at the lamellipodium of chemotaxing T cells. Spatially restricted activation of Ras at the leading edge of amoeboid migrating cells during chemotaxis has also been shown in the slime mold *Dictyostelium*. In *Dictyostelium*, Ras directly regulates PI3K activity at the leading edge, and thus local production of $PI(3,4,5)P_3$, which is essential for the establishment and maintenance of cell polarity and directional movement (Sasaki *et al*, 2004, 2007). Only very little information is available on the function of MEK in *Dicytostelium* chemotaxis (Mendoza *et al*, 2007). Our data revealed a hitherto unknown function of active MEK in cell migration, which is the control of speed and directionality through the regulation of the actin depolymerizing protein cofilin. Interestingly, the MEK-cofilin module seems to be required primarily for amoeboid migration in 3D environments, whereas interference with Ras inhibited T-cell migration in both 2D and 3D environments. It is, therefore, likely that not only in *Dictyostelium*, but also in human T cells, Ras controls—besides the MEK-cofilin pathway—a basic migration module, which is required for directed cell migration in general. Whether also in T cells this involves PI3K is still unclear (Ward, 2004; Ward and Marelli-Berg, 2009). However, in our experiments, transfection of primary human T cells with dominant-negative N17-Ras did not inhibit PI3K activation after SDF-1α treatment. As, in addition, inhibition of PI3K activity did not reduce chemotactic migration in both 2D and 3D environments (see Supplementary Figure S10), this argues against a function of PI3K in an Ras-controlled basic migration programme in human T cells.

Besides the activation of the small GTPase Ras, GPCR triggering also stimulates the activity of the GTPase RhoA (Laudanna *et al*, 1996), which leads to the activation of the protein kinase ROCK (Maekawa *et al*, 1999). ROCK regulates both myosin light chain phosphorylation (Amano *et al*, 1996), thus increasing contractions of the actomyosin system,

and activation of LIMK (Maekawa *et al*, 1999), thus counteracting cofilin dephosphorylation. Interestingly, RhoA as well as ROCK localize at the side and the rear of migrating T cells (Smith *et al*, 2003), thereby restricting actomyosin contractions to the cell body (mid-zone). It is tempting to speculate that ROCK may simultaneously maintain cofilin in its

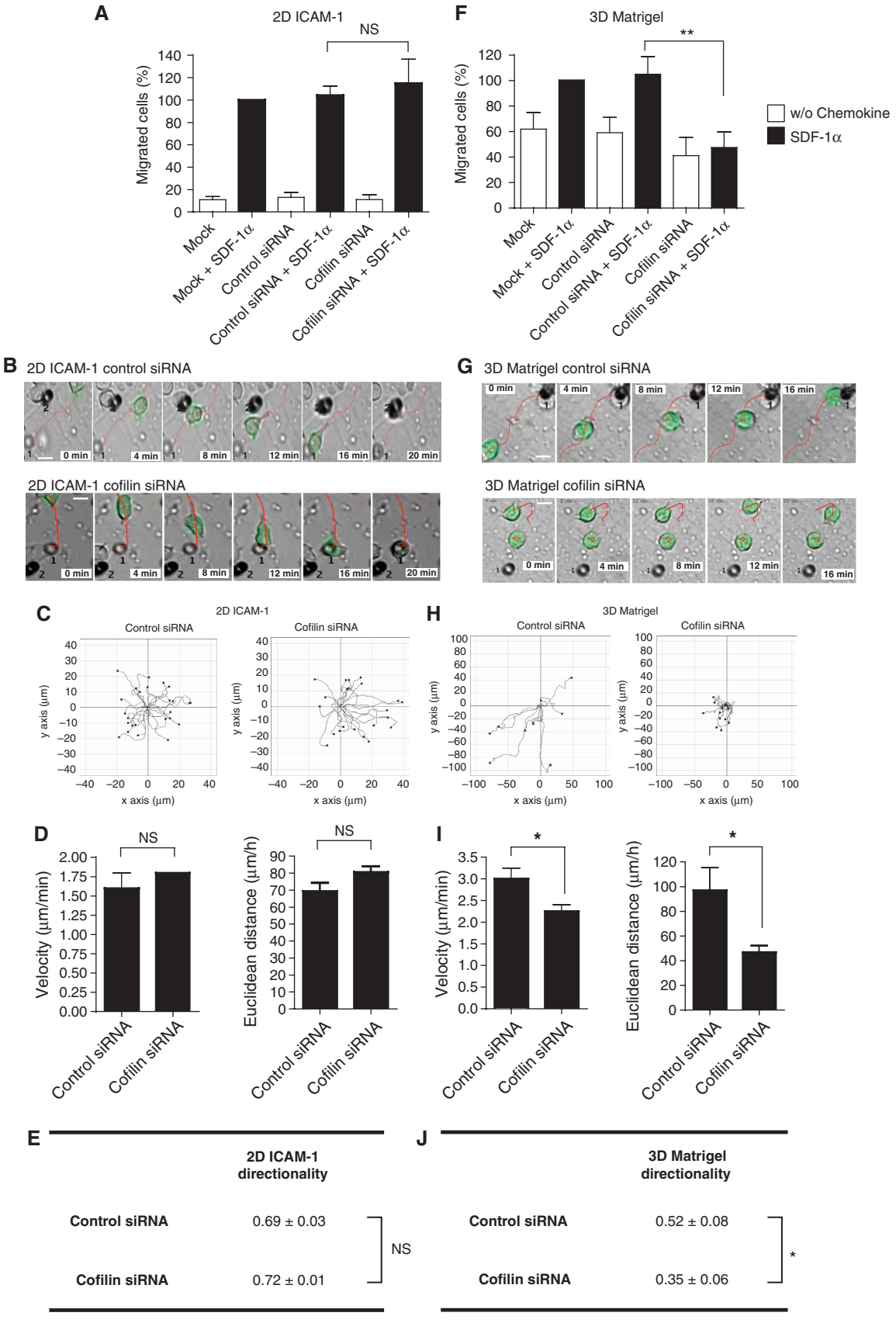

phosphorylated state at the side and the rear of migrating T cells to prevent formation of additional lateral lamellipodial protrusions. In line with this assumption, the front–back axis of migrating T cells is disturbed and polarity gets lost, if dephosphorylation of cofilin at the lamellipodium is prevented, for example through inhibition of MEK. This results in the uncontrolled formation of additional cell protrusions at lateral sides. Of note, in other cell systems, activation of Ras and/or MEK leads to inhibition of the Rho pathway (Sahai *et al*, 2001; Pawlak and Helfman, 2002; Lee and Helfman, 2004). Thus, restricted activation of Ras at the lamellipodium likely simultaneously switches off the Rho pathway at this site, thereby limiting activation of both ROCK and LIMK, to the lateral sides and the uropod of amoeboid migrating T cells.

Interestingly, the phenotype of Cdc42 (another small GTPase) knockout mouse dendritic cells (Lammermann *et al*, 2009) strikingly resembles the phenotype of cofilin knockdown human T cells within the 3D ECM matrix ('multidirectional irritation'; see Figure 10B). Given that Cdc42 is a known regulator of LIM kinase (Edwards *et al*, 1999), it is likely that the phenotype of the Cdc42 knockout cells relies on dysregulated cofilin. As SDF-1α activates Cdc42 also within T cells (del Pozo *et al*, 1999; Haddad *et al*, 2001; Takesono *et al*, 2004), it is tempting to speculate that, besides Ras and MEK, a number of different signalling pathways converges upon cofilin to maintain cell polarity during 3D migration.

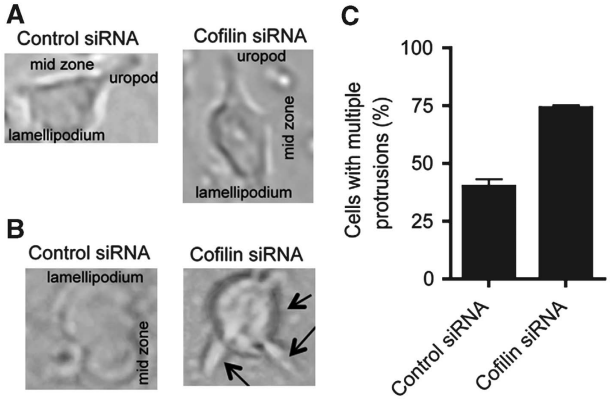

Figure 10 Knockdown of cofilin leads to uncontrolled formation of cell protrusions and thus to a loss of polarity in 3D environments. (**A**, **B**) Human Jurkat T cells were transfected with siRNA as described above, and morphologically analysed by time-lapse videomicroscopy. T cells transfected with the control siRNA (control siRNA) as well as T cells transfected with the cofilin-specific siRNA (cofilin siRNA) display the typical 'hand-mirror-like' morphology of polarized migrating T cells when migrating on a 2D substrate (**A**). T cells transfected with the control siRNA show a single lamellipodial extension (**B**, left panel) at the cell front when migrating within a 3D-Matrigel layer, whereas cells transfected with the cofilin-specific siRNA display many thin processes emanating in all directions (**B**, right panel, black arrows). See also corresponding Supplementary Movie M19. (**C**) A total of 195 control-siRNA-transfected cells and of 227 cofilin-siRNA-transfected cells were analysed for the presence of multiple cell protrusions and impaired migration within the 3D-Matrigel layer. The mean percentage ± s.d. of cells displaying multiple membrane protrusions is shown.

Materials and methods

Transfection of human T cells

Primary human T cells were transfected by nucleofection as described (Klemke *et al*, 2008). Jurkat T cells were transfected through electroporation using the Bio-Rad GenePulser II as described (Klemke *et al*, 2008). For siRNA experiments, 10×10^6 Jurkat T cells in 400 µl PBS containing Ca^{2+} and Mg^{2+} were mixed with 2 µg siRNA and electroporated at 230 V and 950 µF. Thereafter, cells were transferred into 30 ml RPMI 1640 containing 10% FCS and incubated for 72 h at 5% CO_2 and 37°C.

Determination of the phospho-index of cofilin

The phosphorylation state of cofilin was determined as described (Nebl *et al*, 2004; Wabnitz *et al*, 2006; Klemke *et al*, 2008). A detailed description of the method can be found in the Supplementary data.

Immunofluorescence staining and confocal laserscan microscopy

Immunofluorescence staining was performed as described (Klemke *et al*, 2008). Samples were examined by confocal laserscan microscopy (Leica DMRBE with TCS NT). Digitized images were stored and processed using Adobe Photoshop CS3 software. A detailed description of the method can be found in the Supplementary data.

2D- and 3D-transwell chemotaxis assays

Chemotactic migration was analysed as described (Klemke *et al*, 2007, 2008). For 2D-chemotaxis assays, transwell inserts with a pore size of 3 µm (Corning) were used. The transwell inserts were coated with ICAM-1 or with a thin film of Matrigel. For 3D-chemotaxis assays, transwell inserts with a pore size of 8 µm coated with a thick gel layer of growth factor-reduced Matrigel were used. Cells in RPMI1640 + 10% FCS were added in the upper compartment of the transwell insert and RPMI1640 + 10% FCS ± 100 ng/ml SDF-1α was added into the lower compartment. Migration was carried out for 90 min at 37°C. Numbers of transmigrated cells were determined by flow cytometry using an internal bead standard.

For time-lapse videomicroscopy of 2D-chemotactic migration, transwell inserts (8 µm pore size) were coated with ICAM-1 or with a thin film of Matrigel. For time-lapse videomicroscopy of 3D-chemotactic migration, transwell inserts coated with a thick gel of Matrigel were used. Alternatively, in some experiments Matrigel

Figure 9 Knockdown of cofilin impairs chemotactic migration of human T cells in 3D but not 2D environments by reducing speed and directionality. (**A**, **F**) Human Jurkat T cells were either transfected without siRNA (mock), or with a 'scrambled' siRNA (control siRNA) or with a cofilin-specific siRNA (cofilin siRNA). Chemotactic migration across transwell inserts (**A**) or through Matrigel on top of a transwell insert (**F**) was carried out 72 h after transfection. The numbers of mock-transfected cells, which migrated in the presence of SDF-1α (mock + SDF-1α) were set 100 and all other values were expressed relative to them (absolute numbers for mock + SDF-1α were 25.37 ± 4.63% (**A**) and 2.97 ± 0.75% (**F**)). The mean values ± s.d. of three (**A**) or five (**F**) independent experiments are shown. NS, not significant; $^{**}P<0.01$. (**B**, **G**) Human T cells were transfected with siRNA as described above. Then, cells were allowed to migrate on either the ICAM-1-coated 2D surface of a cell culture transwell insert (**B**) or within a 3D-Matrigel layer on top of a transwell insert (**G**) in the presence of SDF-1α in the lower compartment, and time-lapse videomicroscopy was performed. The pores of the transwell insert (source of the chemokine gradient) are labelled with numbers. The tracks of the cells are shown in red. See also corresponding Supplementary Movies M15–M18. (**C**, **H**) Multiple tracks of individual migrating T cells. The starting points of the recorded cell tracks were artificially set to the same origin. Data are representative of three independent experiments. (**D**, **I**) Velocities and Euclidean distances of individual T cells were determined. The mean values ± s.d. of three independent experiments are shown. NS, not significant; $^{*}P<0.05$. (**E**, **J**) The directionality of cell migration for each condition was calculated as the Euclidean distance divided by the accumulated distance. NS, not significant; $^{*}P<0.05$.

was directly mixed with T cells and poured into transwell inserts, and allowed to gel for 30 min at 37°C according to the manufacturers' instructions. The gel in the upper compartment was then overlaid with RPMI1640 + 10% FCS, and RPMI1640 + 10% FCS ± 100 ng/ml SDF-1α was added into the lower compartment. Both experimental settings gave similar results.

Time-lapse videomicroscopy

Time-lapse imaging experiments were performed using a fully automated Axiovert 200M inverted fluorescence microscope (Zeiss) equipped with a CoolSNAP HQ CCD camera (Roper Scientific). Image acquisition was performed using the MetaMorph imaging software (Molecular Devices). Time-lapse images were recorded at 15 or 25 s time intervals. The ImageJ 1.41o software (NIH) and the Manual Tracking plug-in (NIH) were used to track cell paths. The Chemotaxis and Migration Tool Version 1.01 plug-in (ibidi Integrated BioDiagnostics) were used for plotting cell tracks and for velocity and distance measurements. Movies were processed using the Adobe Photoshop CS3 software.

Supplementary data

Supplementary data are available at *The EMBO Journal* Online (http://www.embojournal.org).

Conflict of interest

The authors declare that they have no conflict of interest.

References

Affolter M, Weijer CJ (2005) Signaling to cytoskeletal dynamics during chemotaxis. *Dev Cell* **9:** 19–34

Amano M, Ito M, Kimura K, Fukata Y, Chihara K, Nakano T, Matsuura Y, Kaibuchi K (1996) Phosphorylation and activation of myosin by Rho-associated kinase (Rho-kinase). *J Biol Chem* **271:** 20246–20249

Ambach A, Saunus J, Konstandin M, Wesselborg S, Meuer SC, Samstag Y (2000) The serine phosphatases PP1 and PP2A associate with and activate the actin-binding protein cofilin in human T lymphocytes. *Eur J Immunol* **30:** 3422–3431

Arber S, Barbayannis FA, Hanser H, Schneider C, Stanyon CA, Bernard O, Caroni P (1998) Regulation of actin dynamics through phosphorylation of cofilin by LIM-kinase. *Nature* **393:** 805–809

Campbell DJ, Kim CH, Butcher EC (2003) Chemokines in the systemic organization of immunity. *Immunol Rev* **195:** 58–71

Chen J, Martin BL, Brautigan DL (1992) Regulation of protein serine-threonine phosphatase type-2A by tyrosine phosphorylation. *Science* **257:** 1261–1264

Condeelis J (2001) How is actin polymerization nucleated *in vivo*? *Trends Cell Biol* **11:** 288–293

del Pozo MA, Vicente-Manzanares M, Tejedor R, Serrador JM, Sanchez-Madrid F (1999) Rho GTPases control migration and polarization of adhesion molecules and cytoskeletal ERM components in T lymphocytes. *Eur J Immunol* **29:** 3609–3620

Edwards DC, Sanders LC, Bokoch GM, Gill GN (1999) Activation of LIM-kinase by Pak1 couples Rac/Cdc42 GTPase signalling to actin cytoskeletal dynamics. *Nat Cell Biol* **1:** 253–259

Eibert SM, Lee KH, Pipkorn R, Sester U, Wabnitz GH, Giese T, Meuer SC, Samstag Y (2004) Cofilin peptide homologs interfere with immunological synapse formation and T cell activation. *Proc Natl Acad Sci USA* **101:** 1957–1962

Friedl P, Borgmann S, Brocker EB (2001) Amoeboid leukocyte crawling through extracellular matrix: lessons from the Dictyostelium paradigm of cell movement. *J Leukoc Biol* **70:** 491–509

Friedl P, Entschladen F, Conrad C, Niggemann B, Zanker KS (1998) CD4+ T lymphocytes migrating in three-dimensional collagen lattices lack focal adhesions and utilize beta1 integrin-independent strategies for polarization, interaction with collagen fibers and locomotion. *Eur J Immunol* **28:** 2331–2343

Friedl P, Weigelin B (2008) Interstitial leukocyte migration and immune function. *Nat Immunol* **9:** 960–969

Haddad E, Zugaza JL, Louache F, Debili N, Crouin C, Schwarz K, Fischer A, Vainchenker W, Bertoglio J (2001) The interaction between Cdc42 and WASP is required for SDF-1-induced T-lymphocyte chemotaxis. *Blood* **97:** 33–38

Herrmann C, Martin GA, Wittinghofer A (1995) Quantitative analysis of the complex between p21ras and the Ras-binding domain of the human Raf-1 protein kinase. *J Biol Chem* **270:** 2901–2905

Hotulainen P, Paunola E, Vartiainen MK, Lappalainen P (2005) Actin-depolymerizing factor and cofilin-1 play overlapping roles in promoting rapid F-actin depolymerization in mammalian nonmuscle cells. *Mol Biol Cell* **16:** 649–664

Ibarra N, Pollitt A, Insall RH (2005) Regulation of actin assembly by SCAR/WAVE proteins. *Biochem Soc Trans* **33**(Part 6)**:** 1243–1246

Jacobelli J, Bennett FC, Pandurangi P, Tooley AJ, Krummel MF (2009) Myosin-IIA and ICAM-1 regulate the interchange between two distinct modes of T cell migration. *J Immunol* **182:** 2041–2050

Kiuchi T, Ohashi K, Kurita S, Mizuno K (2007) Cofilin promotes stimulus-induced lamellipodium formation by generating an abundant supply of actin monomers. *J Cell Biol* **177:** 465–476

Klemke M, Rafael MT, Wabnitz GH, Weschenfelder T, Konstandin MH, Garbi N, Autschbach F, Hartschuh W, Samstag Y (2007) Phosphorylation of ectopically expressed L-plastin enhances invasiveness of human melanoma cells. *Int J Cancer* **120:** 2590–2599

Klemke M, Wabnitz GH, Funke F, Funk B, Kirchgessner H, Samstag Y (2008) Oxidation of cofilin mediates T cell hyporesponsiveness under oxidative stress conditions. *Immunity* **29:** 404–413

Kucia M, Reca R, Miekus K, Wanzeck J, Wojakowski W, Janowska-Wieczorek A, Ratajczak J, Ratajczak MZ (2005) Trafficking of normal stem cells and metastasis of cancer stem cells involve similar mechanisms: pivotal role of the SDF-1-CXCR4 axis. *Stem Cells* **23:** 879–894

Lammermann T, Bader BL, Monkley SJ, Worbs T, Wedlich-Soldner R, Hirsch K, Keller M, Forster R, Critchley DR, Fassler R, Sixt M (2008) Rapid leukocyte migration by integrin-independent flowing and squeezing. *Nature* **453:** 51–55

Lammermann T, Renkawitz J, Wu X, Hirsch K, Brakebusch C, Sixt M (2009) Cdc42-dependent leading edge coordination is essential for interstitial dendritic cell migration. *Blood* **113:** 5703–5710

Lappalainen P, Drubin DG (1997) Cofilin promotes rapid actin filament turnover *in vivo*. *Nature* **388:** 78–82

Laudanna C, Campbell JJ, Butcher EC (1996) Role of Rho in chemoattractant-activated leukocyte adhesion through integrins. *Science* **271:** 981–983

Lee KH, Meuer SC, Samstag Y (2000) Cofilin: a missing link between T cell co-stimulation and rearrangement of the actin cytoskeleton. *Eur J Immunol* **30:** 892–899

Lee S, Helfman DM (2004) Cytoplasmic p21Cip1 is involved in Ras-induced inhibition of the ROCK/LIMK/cofilin pathway. *J Biol Chem* **279:** 1885–1891

Ley K, Laudanna C, Cybulsky MI, Nourshargh S (2007) Getting to the site of inflammation: the leukocyte adhesion cascade updated. *Nat Rev Immunol* **7:** 678–689

Loike JD, Cao L, Budhu S, Hoffman S, Silverstein SC (2001) Blockade of alpha 5 beta 1 integrins reverses the inhibitory effect of tenascin on chemotaxis of human monocytes and polymorphonuclear leukocytes through three-dimensional gels of extracellular matrix proteins. *J Immunol* **166:** 7534–7542

Machesky LM, Mullins RD, Higgs HN, Kaiser DA, Blanchoin L, May RC, Hall ME, Pollard TD (1999) Scar, a WASp-related protein, activates nucleation of actin filaments by the Arp2/3 complex. *Proc Natl Acad Sci USA* **96:** 3739–3744

Maekawa M, Ishizaki T, Boku S, Watanabe N, Fujita A, Iwamatsu A, Obinata T, Ohashi K, Mizuno K, Narumiya S (1999) Signaling from Rho to the actin cytoskeleton through protein kinases ROCK and LIM-kinase. *Science* **285:** 895–898

Mendoza MC, Booth EO, Shaulsky G, Firtel RA (2007) MEK1 and protein phosphatase 4 coordinate Dictyostelium development and chemotaxis. *Mol Cell Biol* **27:** 3817–3827

Moriyama K, Iida K, Yahara I (1996) Phosphorylation of Ser-3 of cofilin regulates its essential function on actin. *Genes Cells* **1:** 73–86

Nebl G, Fischer S, Penzel R, Samstag Y (2004) Dephosphorylation of cofilin is regulated through Ras and requires the combined

activities of the Ras-effectors MEK and PI3K. *Cell Signal* **16:** 235–243

Niwa R, Nagata-Ohashi K, Takeichi M, Mizuno K, Uemura T (2002) Control of actin reorganization by slingshot, a family of phosphatases that dephosphorylate ADF/cofilin. *Cell* **108:** 233–246

Nombela-Arrieta C, Lacalle RA, Montoya MC, Kunisaki Y, Megias D, Marques M, Carrera AC, Manes S, Fukui Y, Martinez AC, Stein JV (2004) Differential requirements for DOCK2 and phosphoinositide-3-kinase gamma during T and B lymphocyte homing. *Immunity* **21:** 429–441

Ohashi K, Nagata K, Maekawa M, Ishizaki T, Narumiya S, Mizuno K (2000) Rho-associated kinase ROCK activates LIM-kinase 1 by phosphorylation at threonine 508 within the activation loop. *J Biol Chem* **275:** 3577–3582

Pantaloni D, Le Clainche C, Carlier MF (2001) Mechanism of actin-based motility. *Science* **292:** 1502–1506

Pawlak G, Helfman DM (2002) MEK mediates v-Src-induced disruption of the actin cytoskeleton via inactivation of the Rho-ROCK-LIM kinase pathway. *J Biol Chem* **277:** 26927–26933

Pollard TD, Borisy GG (2003) Cellular motility driven by assembly and disassembly of actin filaments. *Cell* **112:** 453–465

Quintela-Fandino M, Arpaia E, Brenner D, Goh T, Yeung FA, Blaser H, Alexandrova R, Lind EF, Tusche MW, Wakeham A, Ohashi PS, Mak TW (2010) HUNK suppresses metastasis of basal type breast cancers by disrupting the interaction between PP2A and cofilin-1. *Proc Natl Acad Sci USA* **107:** 2622–2627

Sahai E, Olson MF, Marshall CJ (2001) Cross-talk between Ras and Rho signalling pathways in transformation favours proliferation and increased motility. *EMBO J* **20:** 755–766

Samstag Y, Eibert SM, Klemke M, Wabnitz GH (2003) Actin cytoskeletal dynamics in T lymphocyte activation and migration. *J Leukoc Biol* **73:** 30–48

Sasaki A, Chun C, Takeda K, Firtel R (2004) Localized Ras signaling at the leading edge regulates PI3K, cell polarity, and directional cell movement. *J Cell Biol* **167:** 505–518

Sasaki AT, Janetopoulos C, Lee S, Charest PG, Takeda K, Sundheimer LW, Meili R, Devreotes PN, Firtel RA (2007) G protein-independent Ras/PI3K/F-actin circuit regulates basic cell motility. *J Cell Biol* **178:** 185–191

Sidani M, Wessels D, Mouneimne G, Ghosh M, Goswami S, Sarmiento C, Wang W, Kuhl S, El-Sibai M, Backer JM, Eddy R, Soll D, Condeelis J (2007) Cofilin determines the migration behavior and turning frequency of metastatic cancer cells. *J Cell Biol* **179:** 777–791

Smith A, Bracke M, Leitinger B, Porter JC, Hogg N (2003) LFA-1-induced T cell migration on ICAM-1 involves regulation of MLCK-mediated attachment and ROCK-dependent detachment. *J Cell Sci* **116** (Part 15)**:** 3123–3133

Stolp B, Reichman-Fried M, Abraham L, Pan X, Giese SI, Hannemann S, Goulimari P, Raz E, Grosse R, Fackler OT (2009) HIV-1 Nef interferes with host cell motility by deregulation of Cofilin. *Cell Host Microbe* **6:** 174–186

Takesono A, Horai R, Mandai M, Dombroski D, Schwartzberg PL (2004) Requirement for Tec kinases in chemokine-induced migration and activation of Cdc42 and Rac. *Curr Biol* **14:** 917–922

Thelen M, Stein JV (2008) How chemokines invite leukocytes to dance. *Nat Immunol* **9:** 953–959

Theriot JA (1997) Accelerating on a treadmill: ADF/cofilin promotes rapid actin filament turnover in the dynamic cytoskeleton. *J Cell Biol* **136:** 1165–1168

von Andrian UH, Mempel TR (2003) Homing and cellular traffic in lymph nodes. *Nat Rev Immunol* **3:** 867–878

Wabnitz GH, Nebl G, Klemke M, Schroder AJ, Samstag Y (2006) Phosphatidylinositol 3-kinase functions as a Ras effector in the signaling cascade that regulates dephosphorylation of the actin-remodeling protein cofilin after costimulation of untransformed human T lymphocytes. *J Immunol* **176:** 1668–1674

Ward SG (2004) Do phosphoinositide 3-kinases direct lymphocyte navigation? *Trends Immunol* **25:** 67–74

Ward SG, Marelli-Berg FM (2009) Mechanisms of chemokine and antigen-dependent T-lymphocyte navigation. *Biochem J* **418:** 13–27

Wolf K, Muller R, Borgmann S, Brocker EB, Friedl P (2003) Amoeboid shape change and contact guidance: T-lymphocyte crawling through fibrillar collagen is independent of matrix remodeling by MMPs and other proteases. *Blood* **102:** 3262–3269

Woolf E, Grigorova I, Sagiv A, Grabovsky V, Feigelson SW, Shulman Z, Hartmann T, Sixt M, Cyster JG, Alon R (2007) Lymph node chemokines promote sustained T lymphocyte motility without triggering stable integrin adhesiveness in the absence of shear forces. *Nat Immunol* **8:** 1076–1085

Yang N, Higuchi O, Ohashi K, Nagata K, Wada A, Kangawa K, Nishida E, Mizuno K (1998) Cofilin phosphorylation by LIM-kinase 1 and its role in Rac-mediated actin reorganization. *Nature* **393:** 809–812

Zheng Y, Kong Y, Goetzl EJ (2001) Lysophosphatidic acid receptor-selective effects on Jurkat T cell migration through a Matrigel model basement membrane. *J Immunol* **166:** 2317–2322